EFFECT OF Co-SUBSTITUTION OF (Bi,Mn) IONS ON STRUCTURAL, MAGNETIC AND DIELECTRIC PROPERTIES OF ($DyFeO_3$) DYSPROSIUM ORTHOFERRITE

H. ANWAR[a*], Y. JAMIL[a], G. MUSTAFA[b], M. U. ISLAM[b], A. SHAKOOR[b], M. I. ARSHAD[c], H. AKHTAR[a], M. R.S ALEEM[c]
[a]*Department of Physics, University of Agriculture Faisalabad, 38040, Pakistan*
[b]*Department of Physics, Bahauddin,Zakariya University Multan, 60800, Pakistan*
[c]*Department of Physics, G.C. University, Faisalabad 38000, Pakistan*

Nanostructures of $Dy_{1-x}Bi_xFe_{1-y}Mn_yO_3$ system (x,y) = (0.00, 0.10, 0.20, 0.30 and 0.40) were synthesized usingsynchronized double ions substitution by micro-emulsion method at room temperature. Structural, magnetic as well as dielectric properties were investigated by X-ray diffraction (XRD), Fourier transform infrared (FTIR) spectroscopy, vibrating sample magnetometer (VSM) and Dielectric measurements respectively. XRD analysis confirms at all samples have orthorhombic structure, and successful substitution of (Bi,Mn) ions into $DyFeO_3$ crystal structure. The physical parameters were measured from XRD data and found the crystallite size was decreased from (54.9 - 36.6nm)by increasing (x, y) = (Bi, Mn) content. FT-IR analysis showed functional groups and chemical interactions of the sample (x,y) = (0.20) corresponding to the Mn-O, Fe-O and Bi-O bands. The magnetic measurements of all the synthesized samples exhibit paramagnetic behaviour at room temperature. Finally the dielectric parameters results such as the dielectric constant, imaginary dielectric constant and tangent loss were studied at different applied frequencies.

(Received May 1, 2017; Accepted September 5, 2017)

Keywords: Micro-emulsion; dysprosium Orthoferrite; X-ray diffraction; Dielectric response, Hysteresis loops

1. Introduction

Nanostructures are attaining significant attention owing to several surprising features that are not exhibited by analogous bulk material.Due to high surface to volume ratio, nanosized materials show extraordinary performance and potential applications in electronic devices, catalysis reactions, sensing and energy conversion as well as storage devices [1].Transition metal oxides nanostructures have outstanding applications due to their intrinsic variable oxidation state. perovskite structure has been widely studied in recent years due to their special properties such as electrical conductivity, magnetism and catalytic activity. In fact, perovskites are metal oxides having general formula ABO_3.Because these oxide can show conductor and semiconductor behaviour[2], they are excellent electrode materials for batteries as well as fuel cells multi- ferroic oxides in recent times have received extensive attention owing to their potential application in multiple-controlled devices based on the magneto-electric effect. Recently, a magnetic field induced anti ferromagnetic state has been observed in $DyFeO_3$ single crystal [3].In this approach, an effort has been made to get better ferroelectric and magnetic properties in antiferromagnetic dysprosium orthoferrite [4]. One of the important tasks is by reducing the particle size of dysprosium orthoferrite, its magnetic moments can be enhanced.In the literature,$DyFeO_3$ have been investigated, for example,lanthanum doped multiferroic $DyFeO_3$which have spin relaxation and dielectric performance of the nanocrystallites [5], while [6] reported the effects of diamagnetic

*Corresponding author: hafeez.anwar@gmail.com

Ga^{+3}replacements for Fe^{+3}ions in dysprosium orthoferrite.The most remarkable characteristic of perovskites and various other nanoparticles of metal oxides is easy tailoring of their properties by substitution technique, in which the required metal ions are incorporated into the crystal lattice.Ion substitution in dysprosium ortho-ferrite (DFO) is believed to be effective and the most convenient way to enhance the ferroelectric and magnetic properties. Nature of dopants and their concentrations significantly altered the electromagnetic properties of such ferrites. In current work, we report the (Bi,Mn) substituted $Dy_{1-x}Bi_xFe_{1-y}Mn_yO_3$ (x,y) = (0.00, 0.10, 0.20, 0.30 and 0.40) nano crystallites prepared by micro-emulsion method. Our major interest is to investigate structural, magnetic and dielectric behavior of the synthesized material.

2. Materials and Methods

2.1. Chemical Used

All the reagents (Dysprosium (III) nitrate hydrate (Dy (NO_3) xH_2O, 99.9%, Sigma Aldrich), Iron (III) nitrate (Fe $(NO_3)_3.9H_2O$ Merck KGA, 99%), Bismuth nitrate ($Bi(NO_3)_3.5H_2O$, 98%) Manganese Chloride ($MnCl_2.4H_2O$) Beijing Huagongelang), Aqueous Ammonia (NH_4OH) 35%) Cetyltrimethyl ammonium bromide (CTAB) ($C_{16}H_{33}$) N (CH_3) $_3Br$, >99.0% and Deionized water) were of analytical grade. These were used without further purification.

2.2. Samples preparation and Equipments

The nano crystallites $Dy_{1-x}Bi_xFe_{1-y}Mn_yO_3$ (x,y) = (0.00, 0.10, 0.20, 0.30 and 0.40) powder were prepared by micro-emulsion procedure. The appropriate amounts of corresponding metal salts were dissolved in deionized water and thoroughly stirred for 6 h on the magnetic hot plate at (60^oC). Aqueous solution of CTAB (100 mL, 0.3M) was used as surfactant. The pH~ 7 values was adjusted by using freshly papered aqueous ammonia solution. After 3h stirring, the obtained precipitates were then rinsed with deionized water. Ultimately water was evaporated in the oven at 95 ^oC and annealing was carried out at 750 ^oC for ~8h in a controlled temperature muffle furnace Vulcan A-550 with heating rate 5 ^oC/min. X-ray diffraction (XRD) patterns were obtained at room temperature using powder samples in an Xpert Pro PANalytical diffractometer with Cu-Kα radiation (λ = 1.54056 Å) at 40 kV and 30 mA. Intensity data were collected by the step counting method (with a scanning speed 0.05°/s) in the 2θ range from 20º-80º. The surface morphology and microstructure of the samples were studied by JSM-6490 JEOL scanning electron microscope (SEM).Fourier transmission infrared (Nexus 470) spectra of the co-substituted (Bi.Mn) = (0.20) sample was recorded in the range of400-1500cm^{-1}.Magnetization of the all samples was measured by vibrating sample magnetometer Lakeshore-7351 at room temperature. Dielectric properties of nano-crystal structure were measured at room temperature using impedance analyzer HIOKI 3532 LCR HITESTER.

2.3 Calculations

The structural parameters such as unit cell volume, crystallite size, bulk density, X-ray densityand porosity were calculated from XRD data using the following equations[7-9].

$$V_{cell} = a \times b \times c \tag{1}$$

$$D = \frac{k\lambda}{B_{(hkl)}\cos\theta} \tag{2}$$

$$\rho_{bulk} = \frac{m}{2\pi r^2 h} \tag{3}$$

$$\rho_{X-ray} = \frac{ZM}{N_A V} \tag{4}$$

$$P\ \% = 1 - \frac{\rho_{bulk}}{\rho_{X-ray}} \tag{5}$$

Where V is the unit cell volume, Z represents 8 molecules per unit cell. Scherer's formula ascribed by equation 3 was used to calculate the crystallite size (D) nm, where, K is the shape factor, λ is the X-ray wavelength and θ is the Bragg's diffraction angle.In the equation 4, N_A is the Avogadro's number (6.02×10^{23}g/mol) and M is the molecular weight of the sample.

3. Results and discussion

3.1. Structural Analysis

Fig.1 showed the XRD pattern of $Dy_{1-x}Bi_xFe_{1-y}Mn_yO_3$ (x,y) = (0.00, 0.10, 0.20, 0.30 and 0.40)synthesized by micro emulsion method. All the diffraction peaks were indentified using Nelson Relay extrapolation technique and were well indexed as (111), (102), (020), (112), (103), (122), (030), (213), (311), (312), (025) and (314) respectively. These peaks are the characteristics peaks of orthorhombiccrystalline structure of $DyFeO_3$ perovskite and match with the standard pattern (Reference code. 00-013-0199). All the above mentioned peaks were observed in all X-ray diffraction patterns. These results confirmed the formation of $Dy_{1-x}Bi_x$ $Fe_{1-y}Mn_yO_3$ pure perovskite structure. Nevertheless the successful substitution of doped metal ions with the parent metal ions was also confirmed by the presence of all the major and minor peaks at same 2θ values. Lattice parameters a' b' and c' are calculated using 'cell software'.

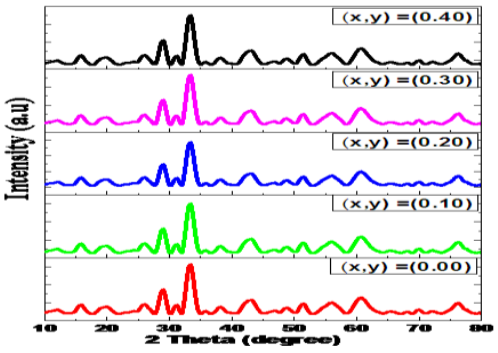

Fig.1. XRD patterns of $Dy_{1-x}Bi_xFe_{1-y}Mn_yO_3$ powder (x,y) =(0.00, 0.10, 0.20, 0.30 and 0.40)

Other parameters like cell volume, crystallite size, x- ray density, porosity were calculatedby using XRD data with the help of aboveequations and their values are given in Table 1.The volume of unit cell can be determined by Eq.1Fig.2 illustrates the behaviour of the unit cell volume along with different (Bi, Mn) concentration. A regular trend was observed by increasing (Bi, Mn) contents, subsequently unit cell volume decreased. It may be attributed due to smaller ionic radii of Bi^{3+} = (1.03 Å) compared to that of Dy^{3+} = (1.05 Å) while Fe^{3+}= (0.64 Å) is replaced with equivalent ionic radii Mn^{3+} = (0.64 Å).Similar behavior has been reported by researchers [10].

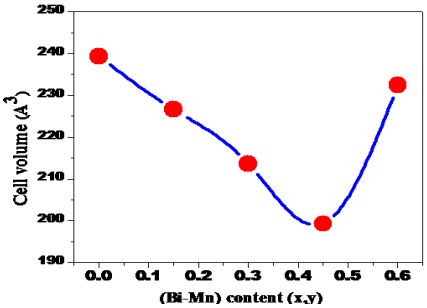

Fig.2.Unit Cell volumes Versus co-substitution (Bi,Mn) content
Table 1. Lattice constants, cell volume, crystallite size, bulk density,

X-ray density and porosity of $Dy_{1-x}Bi_xFe_{1-y}Mn_yO_3$ nanoparticles

Parameters	(x,y) =0.0	(x,y) =0.10	(x,y) =0.20	(x,y)=0.30	(x,y) =0.40
Lattice Constant a (Å)	5.430	5.410	5.359	5.249	5.347
Lattice Constant b (Å)	5.515	5.465	5.438	5.388	5.801
Lattice Constant c (Å)	7.992	7.664	7.331	7.046	7.492
Cell Volume ($Å^3$)	239.353	226.633	213.661	199.289	232.426
Crystallite Size (nm)	54.894	43.868	43.873	43.904	36.561
Bulk density (g/cm^{-3})	4.712	4.241	4.012	3.870	3.823
X-ray density (g/ cm^{-3})	7.396	6.809	8.709	9.565	8.395
Porosity %	36.29	37.72	54	59.6	54.5

The average crystallite size was calculated by using the Scherrer's Eq. 2, and obtained values are listed in Table 1.It is found that behavior of the crystallite size decreases when increasing co-substituted contents. It might be due to the enhancement in surface to volume ratio. The particles size is playing a key role in advanced technological applications. The other physical parameters likeX-ray density; bulk density and porosity were determined by using the Eqs.(3-5) and listed in(Table 1).It was observed that, bulk density was found to be less than X-rays density while porosity is found to be in the range of (36.3-59.6) % which showed porous nature of the material[11].

3.2. Fourier Transform Infrared Spectroscopy

Fig.3 showed that FTIR spectrum of the sample $Dy_{0.8}Bi_{0.2}Fe_{0.8}Mn_{0.2}O_3$powder was recorded in the range 400-1500 cm^{-1}at room temperature. IR spectrum showed, metal-oxides group Bi-O, Mn-O and Fe-O at the frequencies bands 485.9 cm^{-1}, 439.8 cm^{-1} and 423 cm^{-1} respectively, and is in accordance with the previous work reported[12].

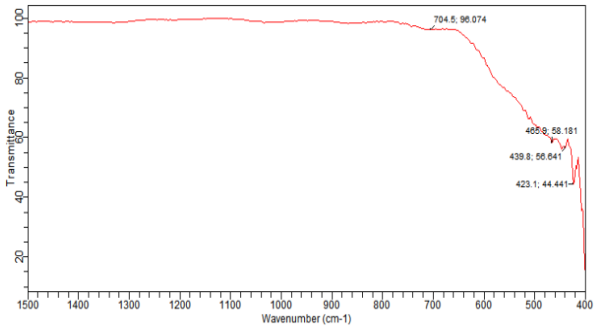

Fig. 3. FTIR spectrum of "$Dy_{1-x}Bi_xFe_{1-y}Mn_yO_3$" perovskite nanoparticles

3.3. Magnetic Properties

The magnetic properties of $Dy_{1-x}Bi_xFe_{1-y}Mn_yO_3$ (x,y) = (0.00,0.10,0.20 and 0.30) nanomaterials were carried out at room temperature. In Fig. 4, all the samples showed that paramagnetic behaviour is observed in which Bi is diamagnetic, while Dy and Mn both are paramagnetic at room temperature whereas Fe is ferromagnetic in nature. There M-H loops parameters, like retentivity, coercivity and magnetization could not be extorted at 298K.

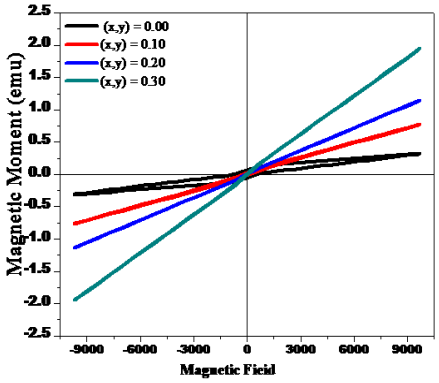

Fig.4. M-H loops showing the evolution of weak ferromagnetic behavior in Co-substituted (Bi,Mn) contents at room temperature

3.4. Dielectric properties

In order to measure the dielectric properties, sample of thickness 1.5 mm was painted with silver paste on both sides and then fired at 200°C for 10 minutes. In the present study, the measurement of capacitance was performed at room temperature while the dielectric constant (ε′), imaginary dielectric part (ε″) and loss tangent (tan δ) were obtained using the recorded data. The samples of ferromagnetic materials made in the form of capacitor are electrically equivalent to the combination of capacitor C_p and resistor R_p, both connected in a parallel combination. The values of the capacitance and the resistance were measured by utilizing impedance analyses, while the dielectric properties were calculated using the following formulae [16-14].

$$\acute{\varepsilon} = \frac{C_o}{C_p} \quad \text{where } C_o = \frac{A\,\varepsilon_0}{d} \tag{6}$$

$$\varepsilon'' = \frac{1}{2\pi f\, C_o R_p} = \acute{\varepsilon} tan\delta \tag{7}$$

$$\tan\delta = \frac{1}{\omega C_p R_p} \tag{8}$$

Wherein Eqs.6,7and 8,$\acute{\varepsilon}$ is the dielectric constant and $\boldsymbol{\varepsilon''}$ is the dielectric loss, A is the area,C is the capacitance, d is the thickness of the pellet, Cp is parallel equivalent capacitance, f is the frequency and Rp is equivalent parallel resistance and ε_o is the permittivity constant.

3.4.1. Dielectric Constant

The dielectric constant **ε'** is defined as "the electrostatic energy stored per unit volume". It can also be defined as, the ratio of the permittivity of a substance to the permittivity of free space. The relative speed of an electromagnetic signal in a material can be measure by using the value of dielectric constant of that material. Fig.5 shows the plot of dielectric constant in the frequency range1 MHz-3GHz at room temperature. The dielectric constant values were measured by using Eq.6 and observed that the dielectric constant **ε'** increases gradually by increasing frequency, then further increase in frequency the dielectric constant values start to become decrease. In these oxides, electric dipoles, dielectric constant **ε'** increase with respect to dielectric relaxation and dielectric polarization [15].

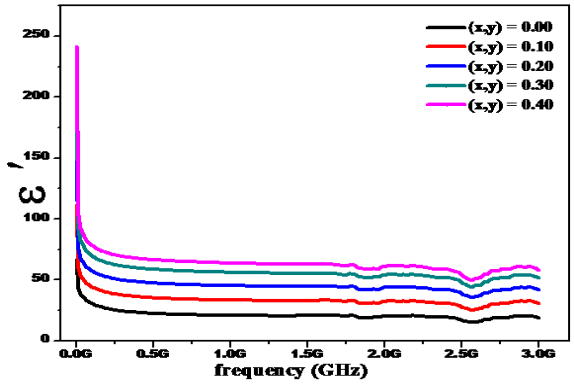

Fig. 5 Effect of frequency on the dielectric constant of $Dy_{1-x}Bi_xFe_{1-y}Mn_yO_3$ nanoparticles (x,y) =(0.00, 0.10, 0.20, 0.30 and 0.40)

The hopping between $Fe^{2+}$and Fe^{3+} ions and Maxwell-Wagner model can be used to explain the decrease in dielectric constant [16]. According to Maxwell-Wagner model, there are two layers which made the dielectric structure of ferrites. The first is the conducting layer which contains the large number of grains while second is the poor conducting layer which contains the grain boundaries. Koop's phonological theory can also explained the resonance peaks which may be attributed due to the electric dipole polarization and interfacial polarization. The resonance peaks may also appear due to the matching of hopping frequency to the applied frequency [17].

3.4.2. Dielectric loss factor

Fig.6 shows the plot of dielectric loss factor **ε"** which gives the energy loss in a dielectric material through the conduction in the frequency range 1 MHz-3GHz. This shows that two resonance peaks that are attributed to the hopping mechanism observed in the frequency range1.6 GHz to 3 GHz. These peaks may appear due to the electric dipole polarization and interfacial polarization [17-18].

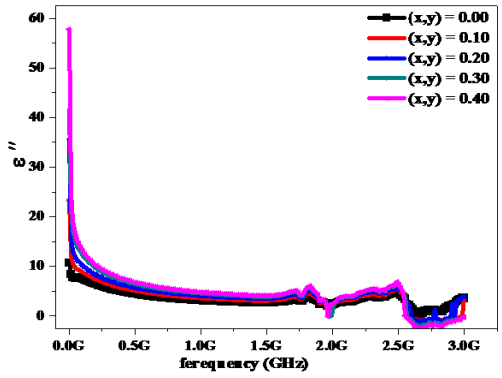

Fig. 6. Effect of frequency on the dielectric loss of $Dy_{1-x}Bi_xFe_{1-y}Mn_yO_3$ nanoparticles (x,y) =(0.00, 0.01, 0.20, 0.30 and 0.40)

3.4.3. Tangent loss

The ratio between the loss current and the charging current in a material is called tangent loss. Fig.7 shows plot of tangent loss is almost invariant with the increasing of frequency from 1 MHz to 1.6 GHz.

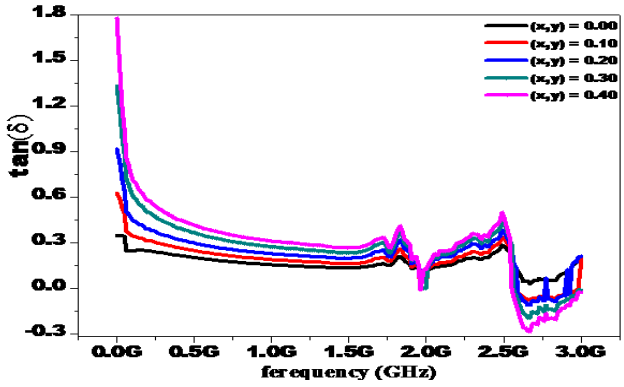

Fig.7. Effect of frequency on the tangent loss of $Dy_{1-x}Bi_xFe_{1-y}Mn_yO_3$ nanoparticles. (x,y) = (0.00, 0.10, 0.20, 0.30 and 0.40)

The resonance peaks have been observed with the increasing frequency from 1.6 GHz to 3 GHz. These resonance peaks may be due to the hopping of electrons which produce the conduction mechanism at the octahedral sites between ferric (Fe^{3+}) and ferrous (Fe^{2+}) ions [19].

4. Conclusions

In the present work, $Dy_{1-x}Bi_xFe_{1-y}Mn_yO_3$ (x,y) = (0.00, 0.10, 0.20, 0.30 and 0.40) were synthesized by micro-emulsion technique. The observed X-ray diffraction parameters show that all synthesized samples are highly crystalline and have pure phase. The effect of increasing co-substituent (Bi,Mn) content reveals that the X-rays density is relatively higher than that of bulk density. Both densities shows the increasing trend, whereas, the porosity has been increased by incorporation of (Bi,Mn) ions. FTIR spectroscopy was also used to investigate chemical interactions and functional groups of prepared samples. Moreover the magnetic parameters exhibit the synthesised samples have paramagnetic behaviour. The low dielectric loss materials are useful in high frequency devices fabrication.

Acknowledgements

The authors are highly thankful to Higher Education Commission (HEC) of Pakistan for providing financial support to carry out this work.

References

[1] C. Burda, X. Chen, R. Narayanan, M.A. El-Sayed,Chem. Rev.105,1025 (2005).
[2] Y. Sun, S. Gao and Y. Xie,Chem. Soc. Rev. 43,530 (2014)
[3] J. Xu,Q. Wang,X. Wang,Q. Xiang,B. Liang, D. Chen, G. Shen, 7(6),5453 (2013).
[4] Y. Du, Z. X. Cheng, X. L. Wang, and S. X. Dou, J. Appl. Phys.107(9),908 (2010).
[5] A. Jaiswal, Raja Das, Tuhin Maity, and Pankaj Poddar, J.Appl.Phys. 110 (2011) 124301
[6] Z. Anwar, M. A. Khan, A. Mahmood, M. Asghar, I. Shakir, M. Shahid, I. Bibi, M. F. Warsi, J.Magn.Magn.Mater.355, 169 (2014)
[7] B.D. Cullity, Second Edition Addison Wesley Publishing, Co; 42-46(89), 92 (1978).
[8] Ghulam Mustafa, M.U. Islam, Wenli Zhang, Yasir Jamil, Abdul Waheed Anwar, Mudassar Hussain, Mukhtar Ahmad, J. Alloys Comp. 618, 428 (2015)
[9] Ghulam Mustafa, M.U. Islam, Wanli Zhang, Abdul Waheed Anwar,Yasir Jamil,GhulamMurtaza, Ihsan Ali, Mudassar Hussain, Akbar Ali, MukhtarAhmad, J. Magn.Magn.Mate.387, 147 (2015)

[10] D.M.Hemed,A.Al Sharif,O.M.Hemed,J.Magn.Magn.Mater.315,11 (2007).
[11] Javed Ahmad, Muhammad QadeerAwan, Muhammad EhsanMazhar, Muhammad Naeem Ashiq, Physica B **406,**254 (2011)
[12] W.D. Kingery, D.R. Uhlmann, Introduction to Ceramics, New York, Wiley, (1976).
[13] Ghulam Mustafa, M.U. Islam,Wenli Zhang, M.I. Arshad,Yasir Jamil, Hafeez Anwar, G.Murtaza, Mudassar Hussain, and Muktar Ahmad, J. Elect. Mate.**45** (11), 5830 (2016).
[14] N. Amin, M. Imran Arshad, M. U. Islam, A. Ali, K. Mahmood, G. Murtaza, M. Ahmad, G.Mustafa, Digest Journal of Nanomaterials and Biostructures **11(**2), 579 (2016).
[14] M.P.F. Graca, M.G. Ferreira da Silva, A.S.B. Sombra, M.A. Valente, Physica B **396,**62 (2007).
[15] C.G. Koops, Phys. Rev. **38**, 121 (1951).
[16] N. Rezlescu,E. Rezlescu,C.Pasnicu,M.L.Craus, J.Phys.Condens.Matter**6**, 5707(1994).
[17] P.J Harrop, Dielectrics, London Butterworths, (1972).
[18] K.L. Ngai, S.W.Martin,Phys. Rev. B **40,**10550 (1989).
[19] L. John Berchmans, R. KalaiSelvan, P.N. Selva Kumar, C.O. Augustin, J. Magn. Magn.Mater. **279**,103 (2004).